EUROPEAN ORGANIZATION FOR NUCLEAR RESEARCH

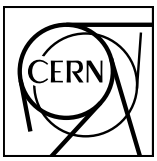

CERN-PH-EP-2010–023
21 July 2010

Quark helicity distributions from longitudinal spin asymmetries in muon–proton and muon–deuteron scattering

The COMPASS Collaboration

Abstract

Double-spin asymmetries for production of charged pions and kaons in semi-inclusive deep-inelastic muon scattering have been measured by the COMPASS experiment at CERN. The data, obtained by scattering a 160 GeV muon beam off a longitudinally polarised NH_3 target, cover a range of the Bjorken variable x between 0.004 and 0.7. A leading order evaluation of the helicity distributions for the three lightest quarks and antiquark flavours derived from these asymmetries and from our previous deuteron data is presented. The resulting values of the sea quark distributions are small and do not show any sizable dependence on x in the range of the measurements. No significant difference is observed between the strange and antistrange helicity distributions, both compatible with zero. The integrated value of the flavour asymmetry of the helicity distribution of the light-quark sea, $\Delta\overline{u} - \Delta\overline{d}$, is found to be slightly positive, about 1.5 standard deviations away from zero.

Keywords: COMPASS, semi-inclusive deep inelastic scattering, spin, structure function, parton distribution functions

(Submitted to Physics Letters B)

The COMPASS Collaboration

M.G. Alekseev[28], V.Yu. Alexakhin[7], Yu. Alexandrov[15], G.D. Alexeev[7], A. Amoroso[27], A. Austregesilo[10,17], B. Badełek[30], F. Balestra[27], J. Barth[4], G. Baum[1], Y. Bedfer[22], J. Bernhard[13], R. Bertini[27], M. Bettinelli[16], R. Birsa[24], J. Bisplinghoff[3], P. Bordalo[12,a], F. Bradamante[25], A. Bravar[24], A. Bressan[25], G. Brona[10,30], E. Burtin[22], M.P. Bussa[27], D. Chaberny[13], M. Chiosso[27], S.U. Chung[17], A. Cicuttin[26], M. Colantoni[28], M.L. Crespo[26], S. Dalla Torre[24], S. Das[6], S.S. Dasgupta[6], O.Yu. Denisov[10,28], L. Dhara[6], V. Diaz[26], S.V. Donskov[21], N. Doshita[2,32], V. Duic[25], W. Dünnweber[16], A. Efremov[7], A. El Alaoui[22], P.D. Eversheim[3], W. Eyrich[8], M. Faessler[16], A. Ferrero[22], A. Filin[21], M. Finger[19], M. Finger jr.[7], H. Fischer[9], C. Franco[12], J.M. Friedrich[17], R. Garfagnini[27], F. Gautheron[2], O.P. Gavrichtchouk[7], R. Gazda[30], S. Gerassimov[15,17], R. Geyer[16], M. Giorgi[25], I. Gnesi[27], B. Gobbo[24], S. Goertz[2,4], S. Grabmüller[17], A. Grasso[27], B. Grube[17], R. Gushterski[7], A. Guskov[7], F. Haas[17], D. von Harrach[13], T. Hasegawa[14], F.H. Heinsius[9], F. Herrmann[9], C. Heß[2], F. Hinterberger[3], N. Horikawa[18,b], Ch. Höppner[17], N. d'Hose[22], C. Ilgner[10,16], S. Ishimoto[18,c], O. Ivanov[7], Yu. Ivanshin[7], T. Iwata[32], R. Jahn[3], P. Jasinski[13], G. Jegou[22], R. Joosten[3], E. Kabuß[13], D. Kang[9], B. Ketzer[17], G.V. Khaustov[21], Yu.A. Khokhlov[21], Yu. Kisselev[2], F. Klein[4], K. Klimaszewski[30], S. Koblitz[13], J.H. Koivuniemi[2], V.N. Kolosov[21], K. Kondo[2,32], K. Königsmann[9], R. Konopka[17], I. Konorov[15,17], V.F. Konstantinov[21], A. Korzenev[22,d], A.M. Kotzinian[27], O. Kouznetsov[7,22], K. Kowalik[30,22], M. Krämer[17], A. Kral[20], Z.V. Kroumchtein[7], R. Kuhn[17], F. Kunne[22], K. Kurek[30], L. Lauser[9], J.M. Le Goff[22], A.A. Lednev[21], A. Lehmann[8], S. Levorato[25], J. Lichtenstadt[23], T. Liska[20], A. Maggiora[28], M. Maggiora[27], A. Magnon[22], N. Makke[22], G.K. Mallot[10], A. Mann[17], C. Marchand[22], A. Martin[25], J. Marzec[31], F. Massmann[3], T. Matsuda[14], W. Meyer[2], T. Michigami[32], Yu.V. Mikhailov[21], M.A. Moinester[23], A. Mutter[9,13], A. Nagaytsev[7], T. Nagel[17], J. Nassalski[30,*], T. Negrini[3], F. Nerling[9], S. Neubert[17], D. Neyret[22], V.I. Nikolaenko[21], A.S. Nunes[12], A.G. Olshevsky[7], M. Ostrick[13], A. Padee[31], R. Panknin[4], D. Panzieri[29], B. Parsamyan[27], S. Paul[17], B. Pawlukiewicz-Kaminska[30], E. Perevalova[7], G. Pesaro[25], D.V. Peshekhonov[7], G. Piragino[27], S. Platchkov[22], J. Pochodzalla[13], J. Polak[11,25], V.A. Polyakov[21], G. Pontecorvo[7], J. Pretz[4], C. Quintans[12], J.-F. Rajotte[16], S. Ramos[12,a], V. Rapatsky[7], G. Reicherz[2], A. Richter[8], F. Robinet[22], E. Rocco[27], E. Rondio[30], D.I. Ryabchikov[21], V.D. Samoylenko[21], A. Sandacz[30], H. Santos[12], M.G. Sapozhnikov[7], S. Sarkar[6], I.A. Savin[7], G. Sbrizzai[25], P. Schiavon[25], C. Schill[9], T. Schlüter[16], L. Schmitt[17,e], S. Schopferer[9], W. Schröder[8], O.Yu. Shevchenko[7], H.-W. Siebert[13], L. Silva[12], L. Sinha[6], A.N. Sissakian[7,*], M. Slunecka[7], G.I. Smirnov[7], S. Sosio[27], F. Sozzi[25], A. Srnka[5], M. Stolarski[10], M. Sulc[11], R. Sulej[31], S. Takekawa[25], S. Tessaro[24], F. Tessarotto[24], A. Teufel[8], L.G. Tkatchev[7], S. Uhl[17], I. Uman[16], M. Virius[20], N.V. Vlassov[7], A. Vossen[9], Q. Weitzel[17], R. Windmolders[4], W. Wiślicki[30], H. Wollny[9], K. Zaremba[31], M. Zavertyaev[15], E. Zemlyanichkina[7], M. Ziembicki[31], J. Zhao[13,24], N. Zhuravlev[7] and A. Zvyagin[16]

[1] Universität Bielefeld, Fakultät für Physik, 33501 Bielefeld, Germany[f]
[2] Universität Bochum, Institut für Experimentalphysik, 44780 Bochum, Germany[f]
[3] Universität Bonn, Helmholtz-Institut für Strahlen- und Kernphysik, 53115 Bonn, Germany[f]
[4] Universität Bonn, Physikalisches Institut, 53115 Bonn, Germany[f]
[5] Institute of Scientific Instruments, AS CR, 61264 Brno, Czech Republic[g]
[6] Matrivani Institute of Experimental Research & Education, Calcutta-700 030, India[h]
[7] Joint Institute for Nuclear Research, 141980 Dubna, Moscow region, Russia[i]
[8] Universität Erlangen–Nürnberg, Physikalisches Institut, 91054 Erlangen, Germany[f]
[9] Universität Freiburg, Physikalisches Institut, 79104 Freiburg, Germany[f]
[10] CERN, 1211 Geneva 23, Switzerland
[11] Technical University in Liberec, 46117 Liberec, Czech Republic[g]
[12] LIP, 1000-149 Lisbon, Portugal[j]
[13] Universität Mainz, Institut für Kernphysik, 55099 Mainz, Germany[f]
[14] University of Miyazaki, Miyazaki 889-2192, Japan[k]

[15] Lebedev Physical Institute, 119991 Moscow, Russia
[16] Ludwig-Maximilians-Universität München, Department für Physik, 80799 Munich, Germany[f,l)]
[17] Technische Universität München, Physik Department, 85748 Garching, Germany[f,l)]
[18] Nagoya University, 464 Nagoya, Japan[k]
[19] Charles University in Prague, Faculty of Mathematics and Physics, 18000 Prague, Czech Republic[g]
[20] Czech Technical University in Prague, 16636 Prague, Czech Republic[g]
[21] State Research Center of the Russian Federation, Institute for High Energy Physics, 142281 Protvino, Russia
[22] CEA IRFU/SPhN Saclay, 91191 Gif-sur-Yvette, France
[23] Tel Aviv University, School of Physics and Astronomy, 69978 Tel Aviv, Israel[m]
[24] Trieste Section of INFN, 34127 Trieste, Italy
[25] University of Trieste, Department of Physics and Trieste Section of INFN, 34127 Trieste, Italy
[26] Abdus Salam ICTP and Trieste Section of INFN, 34127 Trieste, Italy
[27] University of Turin, Department of Physics and Torino Section of INFN, 10125 Turin, Italy
[28] Torino Section of INFN, 10125 Turin, Italy
[29] University of Eastern Piedmont, 1500 Alessandria, and Torino Section of INFN, 10125 Turin, Italy
[30] Sołtan Institute for Nuclear Studies and University of Warsaw, 00-681 Warsaw, Poland[n]
[31] Warsaw University of Technology, Institute of Radioelectronics, 00-665 Warsaw, Poland[n]
[32] Yamagata University, Yamagata, 992-8510 Japan[k]

[a] Also at IST, Universidade Técnica de Lisboa, Lisbon, Portugal
[b] Also at Chubu University, Kasugai, Aichi, 487-8501 Japan[k]
[c] Also at KEK, 1-1 Oho, Tsukuba, Ibaraki, 305-0801 Japan
[d] On leave of absence from JINR Dubna
[e] Also at GSI mbH, Planckstr. 1, D-64291 Darmstadt, Germany
[f] Supported by the German Bundesministerium für Bildung und Forschung
[g] Suppported by Czech Republic MEYS grants ME492 and LA242
[h] Supported by SAIL (CSR), Govt. of India
[i] Supported by CERN-RFBR grants 08-02-91009
[j] Supported by the Portuguese FCT - Fundação para a Ciência e Tecnologia grants POCTI/FNU/49501/2002 and POCTI/FNU/50192/2003
[k] Supported by the MEXT and the JSPS under the Grants No.18002006, No.20540299 and No.18540281; Daiko Foundation and Yamada Foundation
[l] Supported by the DFG cluster of excellence 'Origin and Structure of the Universe' (www.universe-cluster.de)
[m] Supported by the Israel Science Foundation, founded by the Israel Academy of Sciences and Humanities
[n] Supported by Ministry of Science and Higher Education grant 41/N-CERN/2007/0
[*] Deceased

1 Introduction

Measurements of spin asymmetries in polarised Deep Inelastic Scattering (DIS) provide the main source of information on the spin structure of the nucleon. Semi-inclusive DIS (SIDIS) cross-section asymmetries, where in addition to the scattered lepton, pions and kaons are detected, are sensitive to the individual quark and antiquark flavours. Together with DIS and polarised proton–proton data, they are a key ingredient in QCD fits aiming at the evaluation of the quark helicity distributions [1]. Although evaluations of the parton helicity distributions do exist, their uncertainties are still important, particularly for low values of the Bjorken scaling variable x. Data with improved precision, covering a large region of x, should help to clarify several challenging observations made in the last few years. The first one is the flavour asymmetry of the light-quark sea. Unpolarised lepton scattering [2–4], later confirmed by Drell–Yan production experiments [5, 6], has revealed that the light-quark difference, $\overline{u}-\overline{d}$, is negative and much larger in absolute value than expected, resulting in a large violation of the Gottfried sum rule [7]. Model calculations that explain this asymmetry also provide predictions [8–10] for the polarised flavour asymmetry, $\Delta\overline{u}-\Delta\overline{d}$.

The total contribution of the strange quarks, Δs, to the nucleon spin is presently another intriguing issue. Assuming $\mathrm{SU(3)_f}$ flavour symmetry, global fits [11, 12] on inclusive DIS data favour a large and negative first moment for the strange contribution, $\Delta s+\Delta\overline{s}\approx -0.10$. Combined analysis of parity violating $\vec{e}p$ asymmetries and νp elastic data, used for the extraction of the strange axial form factor, also suggests a negative strange quark contribution [13]. Surprisingly, these results are at variance with the most recent determinations of the strange quark distribution $\Delta s(x)$ from SIDIS, which appears to be compatible with zero [14] or even slightly positive [15], at least in the x range of the measurements. Among possible explanations for this observation, a substantial breaking of the $\mathrm{SU(3)_f}$ symmetry has been advocated [16]. The distribution of $\Delta s(x)$ may also change sign at lower values of x. This option is used in a global fit to DIS, SIDIS and proton–proton data [1] to reconcile the medium-x SIDIS data with a large and negative first moment. The dependence of the results on the Fragmentation Functions (FF) and particularly on the strange-quark FF may also introduce a significant bias [17] and for this reason must be quantified. Finally, phenomenological studies usually assume that the strange and antistrange quark helicity distributions are identical, an assumption which has never been tested experimentally. For these reasons a determination of both the shape and the magnitude of the flavour-separated quark helicity distributions is necessary, particularly towards lower values of x.

The first measurements of SIDIS asymmetries were performed by the EMC Collaboration more than twenty years ago [18]. More recently, the SMC Collaboration has measured SIDIS asymmetries for unidentified charged hadrons [19]. The HERMES Collaboration has reported SIDIS asymmetries for charged pion production on a proton target and for charged pion and kaon production on a deuteron target [14]. These asymmetries were used for a flavour decomposition into five helicity distributions. However the data did not permit an extraction of $\Delta\overline{s}$. In a previous publication, we have presented a leading-order (LO) evaluation of the isoscalar polarised valence, sea and strange distributions, $\Delta u_v+\Delta d_v$, $\Delta\overline{u}+\Delta\overline{d}$ and $(\Delta s+\Delta\overline{s})/2$, all derived from DIS and SIDIS asymmetries on a polarised deuteron target only [17].

In this Letter we present new semi-inclusive asymmetries for scattering of high-energy muons off a polarised proton target for production of identified charged pions ($A_{1,p}^{\pi+}$, $A_{1,p}^{\pi-}$) and, for the first time, of identified charged kaons ($A_{1,p}^{K+}$, $A_{1,p}^{K-}$). To the current measurements we have added our previous ($A_{1,d}^{\pi+}$, $A_{1,d}^{\pi-}$) and ($A_{1,d}^{K+}$, $A_{1,d}^{K-}$) SIDIS deuteron data as well as our inclusive double-spin asymmetries $A_{1,p}$ [20] and $A_{1,d}$ [17]. Using these measurements we perform a full flavour decomposition in LO, thus accessing for the first time all up, down and strange quark and antiquark helicity distributions separately.

2 Data

The data presented below were collected in 2007 using the COMPASS spectrometer [21] at CERN. A 160 GeV muon beam was scattered off a polarised NH_3 (ammonia) target. The target consists of three consecutive cells with a length of 30 cm, 60 cm and 30 cm respectively, polarised by Dynamic Nuclear Polarisation (DNP). Neighbouring target cells were always polarised in opposite directions. The spin orientations were reversed once per day by rotating the solenoidal magnetic field and, in addition, every few weeks by interchanging the DNP microwave frequencies. The beam and target polarisations of -0.80 and about ± 0.90 are known with relative precisions of 5% and 2%, respectively. The energy of the incident muons was constrained to be in the interval 140 GeV $< E_\mu <$ 180 GeV. The kinematic region was defined by cuts on the photon virtuality, $Q^2 > 1$ (GeV/c)^2, and on the fractional energy, y, transfered from the incident muon to the virtual photon $0.1 < y < 0.9$. The selected data sample covers the range $0.004 < x < 0.7$ and consists of 85.3 million events.

The reconstruction procedure is described in Ref. [22]. All events were required to have a reconstructed primary vertex inside one of the target cells. Only hadron tracks originating from the primary vertex were considered. Their fractional energy, z, was required to be larger than 0.2 in order to select hadrons produced in the current fragmentation region and smaller than 0.85 in order to suppress hadrons originating from diffractive processes. Tracks crossing more than 30 radiation lengths were not accepted as hadrons. Hadrons were identified in the RICH detector. The momentum range was restricted to the interval 10 GeV/$c < p <$ 50 GeV/c where both pions and kaons can be identified. The measured RICH photoelectron distributions were compared to parameterisations calculated using the pion and kaon masses, taking into account the observed background. The masses of the detected hadrons were then assigned according to their likelihood ratios. The total samples of π^+, (π^-) and K^+ (K^-) amount to 12.3 (10.9) and 3.6 (2.3) million hadrons, respectively.

Since the RICH detector does not select pure samples of pions and kaons, a correction accounting for the fraction of misidentified hadrons in each sample was applied. The unfolding procedure is the same as that used for the ^{6}LiD data in Ref. [17]. The purity of the pion samples selected by the RICH detector is larger than 0.98 over the full range of x, while for kaons it varies from about 0.73 at the lowest value of x to about 0.93 and 0.91 at $x \geq 0.03$ for positive and negative kaons, respectively. The applied unfolding corrections have only a small effect on the pion and kaon asymmetries.

3 Asymmetries

Spin asymmetries were calculated from the numbers of hadrons originating from cells with opposite spin orientations collected before and after a target field rotation so that flux and acceptance factors cancel out. Corrections were applied for QED radiative effects [23] and for the polarisation of the ^{14}N nucleus. The latter is proportional to the corresponding asymmetry for a deuteron target and approximately given by [24]:

$$\Delta A^h_{1,p} = \frac{1}{3} \cdot (-\frac{1}{3}) \cdot \frac{1}{6} \cdot \frac{\sigma^h_d(x)}{\sigma^h_p(x)} \cdot A^h_{1,d}(x) \tag{1}$$

where $h = \pi^+, \pi^-, K^+, K^-$. The factors account for the fraction of polarisable nitrogen nucleons in ammonia, the alignment of the proton spin vs. the ^{14}N spin, the ratio of ^{14}N to ^{1}H polarisations and the ratio of the hadron cross sections, σ^h_d and σ^h_p, for scattering of muons off unpolarised deuteron and proton targets. The correction thus varies both with x and the type of hadron: for π^+, π^- and K^+ it reaches about -0.015 at $x = 0.5$, while for K^- it remains practically equal to zero due to the vanishing values of $A^{K^-}_{1,d}$.

The semi-inclusive virtual-photon asymmetries for scattering of muons off a proton target are listed in Table 1 with their statistical and systematic errors. Since inclusive and semi-inclusive asymmetries

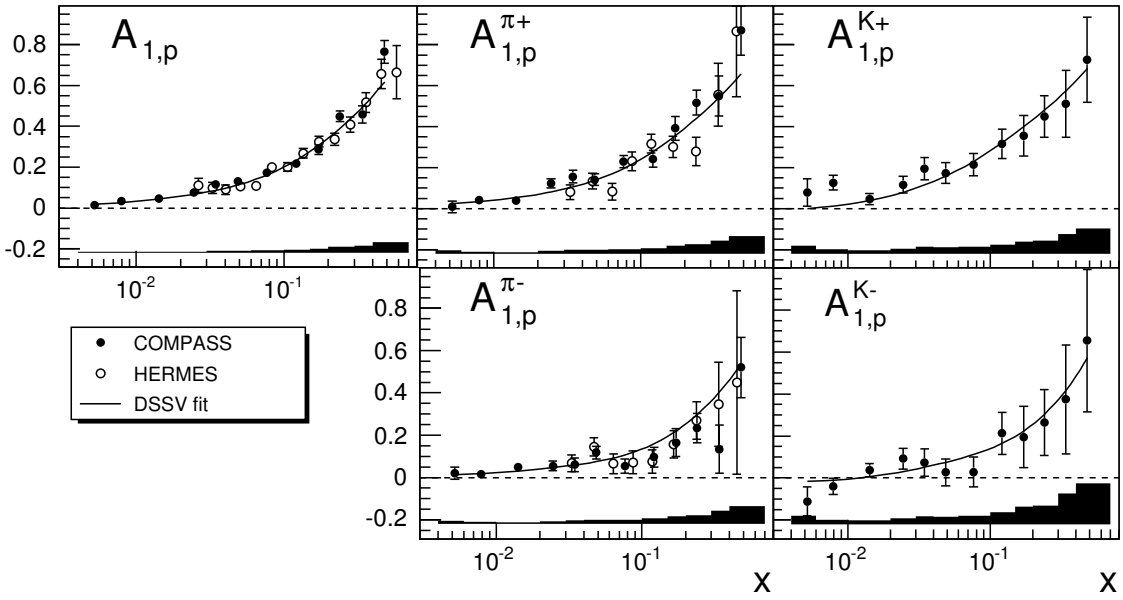

Fig. 1: The inclusive asymmetry $A_{1,p}$ [20] and the semi-inclusive asymmetries $A_{1,p}^{\pi+}$, $A_{1,p}^{K+}$, $A_{1,p}^{\pi-}$, $A_{1,p}^{K-}$ from the present measurements (closed circles). The bands at the bottom of each plot show the systematic errors. The $A_{1,p}$, $A_{1,p}^{\pi+}$ and $A_{1,p}^{\pi-}$ measurements from HERMES [14, 26] (open circles) are shown for comparison. The curves show the predictions of the DSSV fit [1].

originate from the same events, their errors are correlated (see Table 2). The largest correlations (≈ 0.4) are those between inclusive and semi-inclusive pion asymmetries, due to the larger pion multiplicity. The unfolding procedure also generates a negative correlation between pions and kaons of the same charge. This correlation is larger at small x (≈ -0.16) due to the lower purity of the kaon sample.

The systematic errors contain a multiplicative part resulting from uncertainties of the beam and target polarisations, the dilution factor and the ratio $R = \sigma^L/\sigma^T$ used to calculate the depolarisation factor [25]. Added in quadrature, these uncertainties amount to 6% of the value of the asymmetry. An important contribution to the systematic error arises from possible false asymmetries generated by instabilities in the experimental setup. The effect of these random instabilities was evaluated by a statistical test on the asymmetries made on 23 subsets of data. At the level of one standard deviation the upper bound of the error due to these time-dependent effects is found to be $0.56\sigma_{stat}$.

The experimental double-spin asymmetries for a proton target are shown in Fig. 1. They are compared to the predictions of the DSSV fit [1] at the (x, Q^2) values of the data. The HERMES inclusive [26] and semi-inclusive [14] measurements for π^+ and π^- are also displayed. The agreement with the DSSV parameterisation is good, even for the kaon asymmetries for which no data were available when the prediction was made. In spite of the different kinematic conditions, the agreement between the COMPASS and the HERMES values for the pion asymmetries is also good. This observation illustrates the fact that the Q^2 dependence at fixed x is small for semi-inclusive asymmetries.

The spin asymmetries for a deuteron target were evaluated from our previous data obtained with a ^{6}LiD target. The published values [17] were corrected to account for the admixtures of ^{7}Li (4.4%) and ^{1}H (0.5%) in the target material [27]. These isotopes are both polarised to more than 90% [28]. The resulting corrections, which do not exceed one fourth of the statistical error, are listed in Table 3 for each asymmetry and each bin of x.[1] A similar correction to the inclusive asymmetry $A_{1,d}$ has been used in Ref. [20].

[1] These corrections should always be applied when using the data of Ref. [17].

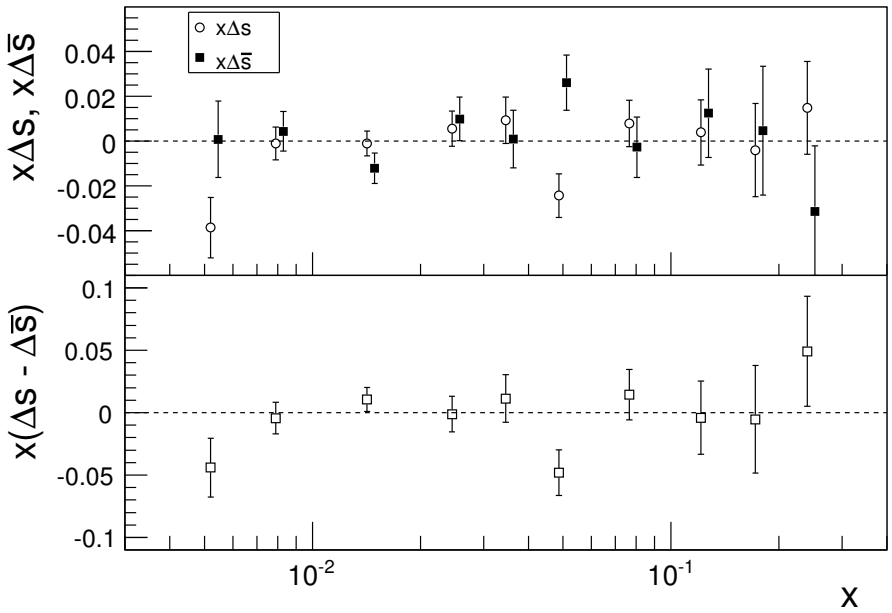

Fig. 2: Comparison of $x\Delta s$ (open circles) and $x\Delta\overline{s}$ (squares) at $Q_0^2 = 3$ (GeV/c)^2 (top) and corresponding values of the difference $x(\Delta s - \Delta\overline{s})$ (bottom).

4 Polarised PDFs from a LO fit to the asymmetries

At LO in QCD and under the assumption of independent quark fragmentation, the spin asymmetry for hadrons h produced in the current fragmentation region can be written as a sum of products of the quark, Δq, and antiquark, $\Delta\overline{q}$, helicity distributions with the corresponding fragmentation functions D_q^h and $D_{\overline{q}}^h$:

$$A_1^h(x,z) \;=\; \frac{\sum_q e_q^2\Big(\Delta q(x)D_q^h(z) + \Delta\overline{q}(x)D_{\overline{q}}^h(z)\Big)}{\sum_q e_q^2\Big(q(x)D_q^h(z) + \overline{q}(x)D_{\overline{q}}^h(z)\Big)}\,. \tag{2}$$

In the present analysis the Q^2 dependence of the asymmetries is neglected and all measurements are assumed to be valid at $Q_0^2 = 3$ (GeV/c)^2. The LO unpolarised parton distributions (PDFs) with three quark flavours from the MRST parameterisation [29] are used. The fragmentation functions are taken from the LO parameterisation of DSS [30]. As in previous analyses [17,19], the unpolarised PDFs which are extracted from cross sections assuming non-zero values of R are corrected by a factor $1+R(x,Q_0^2)$ [25] to take into account the fact that R is assumed to be zero at LO. The asymmetries for a deuteron target are corrected by the factor $(1 - 1.5\omega_D)$ where ω_D is the probability for a deuteron to be in a D-state ($\omega_D = 0.05 \pm 0.01$) [31]. The four semi-inclusive asymmetries for a proton target, the four semi-inclusive asymmetries for a deuteron target and the two inclusive asymmetries thus provide a system of ten equations with six unknowns (Δu, Δd, $\Delta\overline{u}$, $\Delta\overline{d}$, Δs and $\Delta\overline{s}$). A least-square fit to the data is performed independently in each bin of x. The analysis is limited to $x \leq 0.3$ because the antiquark distributions become insignificant above this limit. Above $x = 0.3$, $\Delta u(x)$ and $\Delta d(x)$ are obtained from the inclusive structure functions $g_1^p(x)$ and $g_1^d(x)$ by assuming $\Delta\overline{q}$ to be zero.

The fit results for the Δs and $\Delta\overline{s}$ distributions and for their difference are displayed in Fig. 2. In the measured x range both distributions are flat and compatible with zero. The same observation can be made for their difference, $\Delta s - \Delta\overline{s}$; only one point out of ten is outside two standard deviations (2.7 σ at $x = 0.0487$). We have checked that the vanishing values of $\Delta s - \Delta\overline{s}$ are not artificially generated by the MRST parameterisation of the unpolarised PDFs where $s(x) = \overline{s}(x)$ is assumed. The $s(x)$ and $\overline{s}(x)$ distributions were scaled simultaneously by factors 2 and 0.5 and allowed to differ in any interval of x by a factor of 2. The values of $\Delta s(x)$ and $\Delta\overline{s}(x)$ were found to be nearly independent of these modifications.

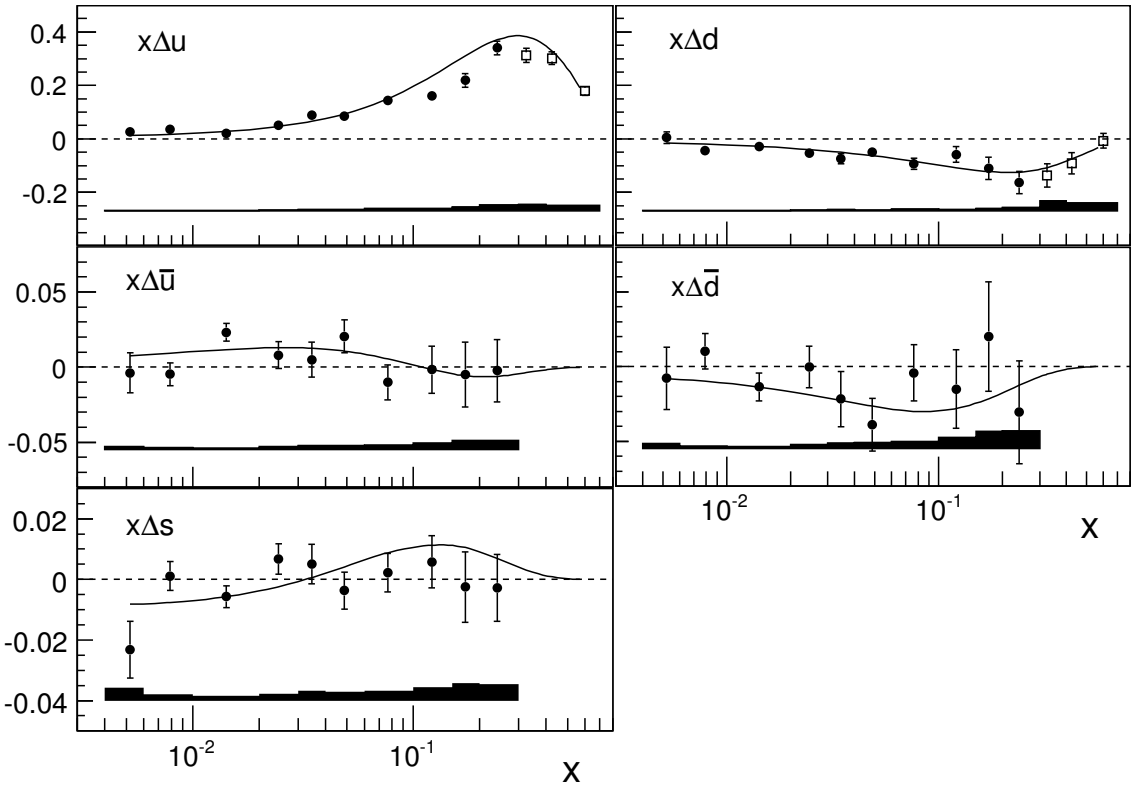

Fig. 3: The quark helicity distributions $x\Delta u$, $x\Delta d$, $x\Delta\overline{u}$, $x\Delta\overline{d}$ and $x\Delta s$ at $Q_0^2 = 3$ (GeV/c)^2 as a function of x. The values for $x < 0.3$ (black dots) are derived at LO from the COMPASS spin asymmetries using the DSS fragmentation functions [30]. Those at $x > 0.3$ (open squares) are derived from the values of the polarised structure function $g_1(x)$ quoted in [20,35] assuming $\Delta\overline{q} = 0$. The bands at the bottom of each plot show the systematic errors. The curves show the predictions of the DSSV fit calculated at NLO [1].

We conclude that there is no significant difference between $\Delta s(x)$ and $\Delta\overline{s}(x)$ in the x-range covered by the data. This conclusion remains valid when the DSS fragmentation functions used in the fit are replaced by those derived by EMC [32]. The results on $\Delta s(x)$ and $\Delta\overline{s}(x)$ are at variance with the SU(3) Chiral Quark-Soliton model prediction $|\Delta s(x)| \gg |\Delta\overline{s}(x)|$ [33] but are compatible with statistical models predicting that $\Delta s(x) - \Delta\overline{s}(x)$ should be zero [8] or small [34].

From here on the distributions of Δs and $\Delta\overline{s}$ will be assumed to be equal, an assumption which reduces the number of unknowns to five and improves the statistical precision of the fit results at least by a factor 1.5. The χ^2 of the fits varies from 1.8 to 8.5 in the different x bins with an average of 4.0 for 5 degrees of freedom, corresponding to a probability of 55%. Within their statistical precision the data are thus compatible with the factorisation formula of Eq. (2).

The results for the quark helicity distributions Δu, Δd, $\Delta\overline{u}$, $\Delta\overline{d}$ and Δs ($\Delta s = \Delta\overline{s}$) are shown in Fig. 3. As for the asymmetries, they are in good qualitative agreement with the results from HERMES [14]. A quantitative comparison is not made here, since the HERMES helicity distributions are extracted under different assumptions for the fragmentation functions and for the unpolarised flavour distributions. In the range $0.3 < x < 0.7$ three additional values of Δu and Δd, derived from the $g_1^p(x)$ and $g_1^d(x)$ [35] structure functions, are also displayed. The $g_1^d(x)$ values include the target material corrections quoted in [20]. The dominant contribution to the systematic error of Δu and Δd comes from the uncertainty of the beam polarisation, which affects all data in the same way and leads to an uncertainty of 5% for all fitted values. The systematic error on the antiquark and strange quark distributions is mainly due to possible false asymmetries generated by time-dependent effects on the detector acceptance. The curves show the results of the DSSV fit at Next-to-Leading Order (NLO) [1]. The comparison with the experimental

results derived at LO is thus only qualitative. Nevertheless, the curves reproduce fairly well the shape of the data, confirming a previous observation that a direct extraction at LO provides a good estimate of the shape of the helicity distributions [36]. The antiquark distributions, $\Delta\overline{u}$ and $\Delta\overline{d}$, do not show any significant variation in the x range of the data, the former being consistent with zero, the latter being slightly negative.

The values of the strange quark helicity distribution confirm with slightly reduced errors the results obtained from the deuteron data [17] alone. With the same fragmentation functions (DSS) no significant variation of $\Delta s(x)$ is observed in the range of the data. Only the first point at low x shows a small deviation from zero ($\approx 2.5\sigma$). This distribution is of special interest due to the apparent contradiction between the SIDIS results and the negative first moment derived [35] from the spin structure function $g_1(x)$. The DSSV fit includes a negative contribution to Δs for $x \leq 0.03$, which reconciles the inclusive and semi-inclusive results. The evaluation of the first moment of $\Delta s(x)$ from inclusive measurements relies on the value of the octet axial charge a_8, which is derived from hyperon weak decays under the assumption of $\mathrm{SU(3)_f}$ symmetry. A recent model calculation suggests that a_8 may be substantially reduced and become close to the singlet axial charge a_0 extracted from the data [16]. In this case the inclusive data would no longer imply a negative value of Δs. Finally, as pointed out in our previous paper [17], one has to keep in mind that the semi-inclusive results on $\Delta s(x)$ strongly depend on the choice of a set of fragmentation functions. This dependence is quantified in the next section.

The first moments of the helicity distributions truncated to the range of the measurements are listed in Table 4. The missing contributions at low and at high x have been evaluated by extrapolating the measured values and alternatively by using the DSSV parameterisation [1]. The contributions at high x are all small and do not exceed 0.01. The two methods lead to similar values for the valence quark moments $\Delta u_v = \Delta u - \Delta\overline{u}$ and $\Delta d_v = \Delta d - \Delta\overline{d}$. In contrast, they differ for the sea quark moments and particularly for Δs due to the sizable low-x contribution assumed in the DSSV fit. The resulting full first moments for both methods are listed in Table 5. The sum of the quark and antiquark contributions $\Delta\Sigma = 0.32 \pm 0.03(stat.)$, obtained by linearly extrapolating the data, is nearly identical to the value of $a_0 = 0.33 \pm 0.03(stat.)$[2] derived [35] from the first moment of $g_1^d(x)$ using the octet axial charge a_8. Not surprisingly, the extrapolation with the DSSV parameterisation results in a much smaller value for $\Delta\Sigma$. The observed difference comes mainly from the negative behaviour of Δs assumed at small x. The sum of the valence quark contributions $\Delta u_v + \Delta d_v = 0.39 \pm 0.03(stat.)$ is also consistent with our previous determination based on the difference asymmetry of positive and negative hadrons in a subsample of the present deuteron data ($0.41 \pm 0.07(stat.)$ at $Q_0^2 = 10\ (\mathrm{GeV}/c)^2$) [37].

The flavour asymmetry of the helicity distribution of the sea, $\Delta\overline{u} - \Delta\overline{d}$, is shown in Fig. 4. Although compatible with zero, the values indicate a slightly positive distribution. The DSSV fit at NLO [1] and the unpolarised asymmetry $\overline{d} - \overline{u}$ are shown for comparison. The first moment $\Delta\overline{u} - \Delta\overline{d}$ truncated to the range $0.004 < x < 0.3$ is $0.06 \pm 0.04(\mathrm{stat.}) \pm 0.02(\mathrm{syst.})$. It is worth noting that the polarised first moment is about one standard deviation smaller than the unpolarised one truncated to the same range (≈ 0.10 for the MRST parameterisation [29]). The data thus disfavour models predicting $\Delta\overline{u} - \Delta\overline{d} \gg \overline{d} - \overline{u}$ (see Refs. [9, 38] and references therein). Three model predictions are shown in Fig. 4. The statistical model of Ref. [10] and the SU(3) version of the Chiral Quark–Soliton model of Ref. [33] both predict positive distributions, while the Meson Cloud model of Ref. [39] predicts a slightly negative distribution. Within the statistical errors, the COMPASS data are compatible with all three predictions. The sum of the light quark helicity distributions, $\Delta\overline{u} + \Delta\overline{d}$, is mainly constrained by the deuteron data and nearly identical to the result published in Ref. [17]. The first moment truncated to the range of the data is found to be $-0.03 \pm 0.03(\mathrm{stat.}) \pm 0.01(\mathrm{syst.})$.

[2] The admixture of ^{7}Li and ^{1}H in the target material reduces the value of a_0 quoted in Ref. [35] by 0.02 [20].

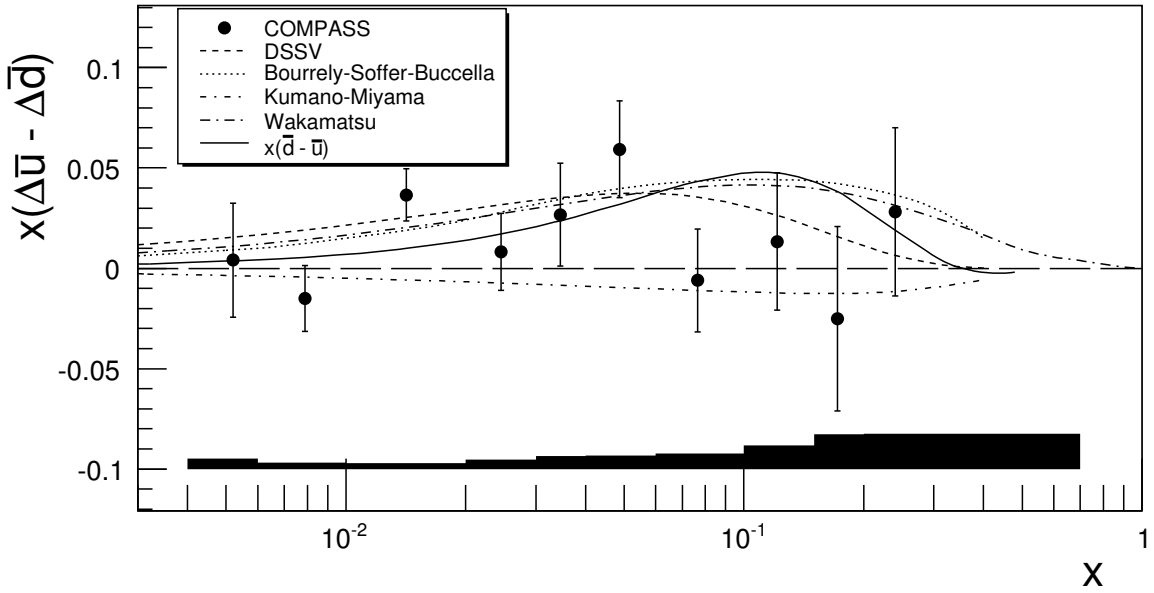

Fig. 4: The flavour asymmetry of the helicity distribution of the sea $x(\Delta\overline{u}-\Delta\overline{d})$ at $Q_0^2 = 3$ (GeV/c)^2. The shaded area displays the systematic error. The dashed curve is the result of the DSSV fit at NLO. The other curves are model predictions from Wakamatsu [33] (long dash-dotted line), Kumano and Miyama [39] (short dash-dotted line) and Bourrely, Soffer and Buccella [10] (dotted line). The solid curve shows the MRST parameterisation for the unpolarised difference $x(\overline{d}-\overline{u})$ at NLO.

5 Influence of the fragmentation functions on the helicity distributions

The relation between the semi-inclusive asymmetries and the quark helicity distributions (Eq. (2)) depends only on the ratios of fragmentation functions integrated over the selected range of z ($0.2 < z < 0.85$). Relevant for the kaon asymmetries are the unfavoured-to-favoured FF ratio, R_{UF}, and strange-to-favoured FF ratio, R_{SF}:

$$R_{UF} = \frac{\int D_d^{K^+}(z)\mathrm{d}z}{\int D_u^{K^+}(z)\mathrm{d}z}, \quad R_{SF} = \frac{\int D_{\bar{s}}^{K^+}(z)\mathrm{d}z}{\int D_u^{K^+}(z)\mathrm{d}z}. \tag{3}$$

In the DSS parameterisation, the R_{UF} and R_{SF} ratios are equal to 0.13 and 6.6 respectively. In the earlier EMC parameterisation [32] R_{SF} is substantially smaller, $R_{SF} = 3.4$, whereas R_{UF} is larger, $R_{UF} = 0.35$. Since the pion fragmentation functions are better constrained by the data than the kaon ones, the effect of the corresponding ratios on the final result is expected to be much smaller. The dependence of the truncated moments quoted in Table 4 was then evaluated by varying R_{SF} from $R_{SF} = 2.0$ to $R_{SF} = 7.0$. In order to keep the K^+ multiplicity approximately constant, the value of R_{UF} was simultaneously varied from 0.45 to 0.10 according to the relation $R_{UF} = 0.35 - 0.07(R_{SF} - 3.4)$. The resulting truncated first moments Δu, $\Delta\overline{u}$, Δd, $\Delta\overline{d}$, Δs and $\Delta\overline{u} - \Delta\overline{d}$ are shown in Fig. 5 as a function of R_{SF}. We observe that the values of Δu ($\Delta\overline{u}$) increase (decrease) by more than one standard deviation when the ratios evolve from the DSS to the EMC values. In contrast both Δd and $\Delta\overline{d}$ remain nearly constant. The variation of Δs is much more pronounced: its value evolves from -0.01 to -0.04, although with a much larger error. The difference $\Delta\overline{u} - \Delta\overline{d}$ follows the same trend as $\Delta\overline{u}$. It slightly decreases with R_{SF}, down to one standard deviation from zero at $R_{SF} = 3.4$. We note that the simultaneous changes of the two ratios, while leaving the K^+ rate practically unchanged, affect the K^- rate only for $x \geq 0.1$. Precise values of R_{UF} and R_{SF} may thus be difficult to extract from the data.

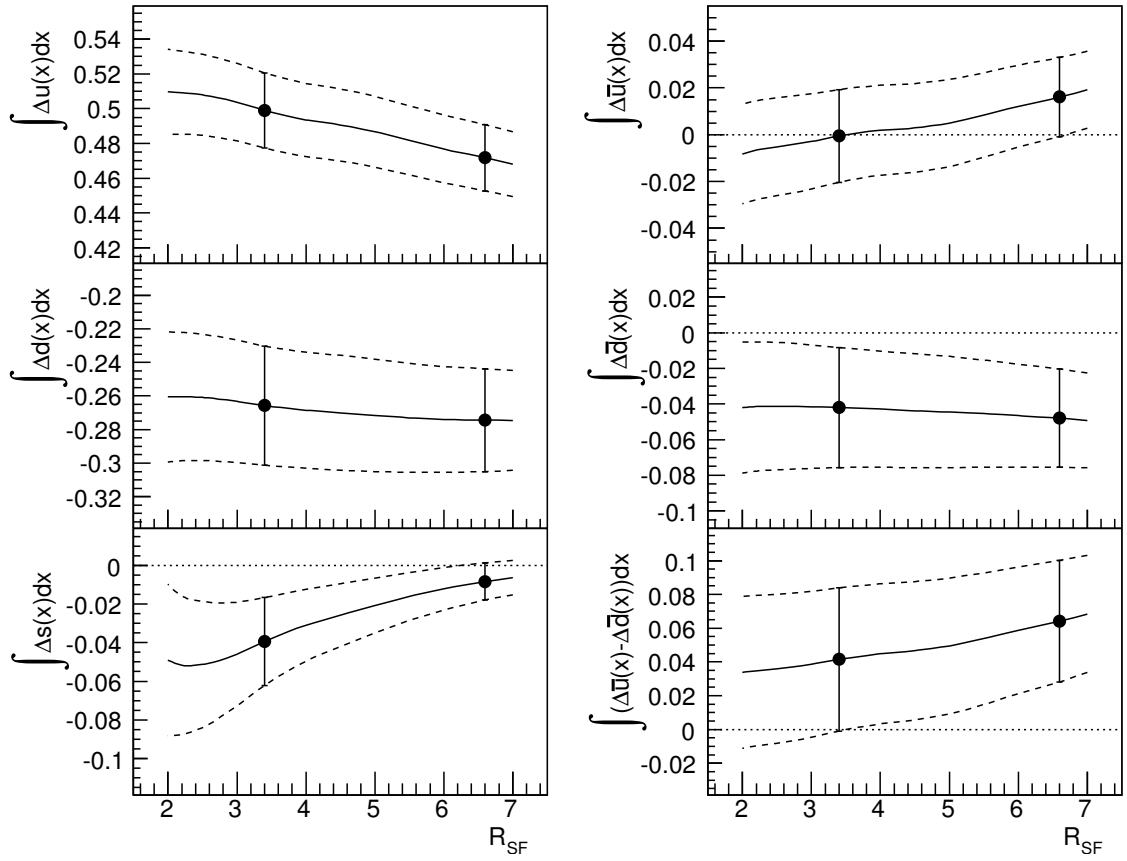

Fig. 5: Variation of the quark first moments Δu, $\Delta\overline{u}$, Δd, $\Delta\overline{d}$, Δs and $\Delta\overline{u}-\Delta\overline{d}$ integrated over the interval $0.004 < x < 0.3$ as a function of the ratio R_{SF} of $\overline{s}$ and u quark fragmentation functions into K^+. The ratio R_{UF} is varied linearly from 0.13 at $R_{SF} = 6.6$ to 0.35 at $R_{SF} = 3.4$. The left and right black points indicate the values obtained using the EMC [32] and the DSS [30] kaon fragmentation functions, respectively.

6 Conclusions

Longitudinal spin asymmetries for identified charged pions and kaons in semi-inclusive muon scattering on a proton target have been measured. The pion data extend the measured region by an order of magnitude towards small x, while the kaon asymmetries for the proton were measured for the first time. The new SIDIS asymmetries for the proton were combined with our previous SIDIS asymmetries for the deuteron and with both proton and deuteron inclusive measurements in order to evaluate the three lightest flavour quark and antiquark helicity distributions. The resulting Δu and Δd distributions are dominant at medium and high x. The values of the antiquark distributions are small and do not show any significant variation in the measured range. The $\Delta\overline{u}$ distribution is consistent with zero, while $\Delta\overline{d}$ seems to indicate a slightly negative behaviour. Accordingly, the flavour asymmetry of the helicity distribution of the sea, $\Delta\overline{u}-\Delta\overline{d}$, is slightly positive, about 1.5 standard deviations from zero. No difference is observed between the Δs and $\Delta\overline{s}$ distributions, which are both compatible with zero over the measured x range. The sum of the flavour-separated first moments, linearly extrapolated to $x = 0$, is in good agreement with our previous determination of $\Delta\Sigma$ based on the first moments of the spin structure function $g_1^d(x)$. The dependence of the results on the fragmentation functions used was evaluated. Sizable for Δu and $\Delta\overline{u}$ distributions, this dependence becomes critical for the Δs distribution.

Acknowledgements

We gratefully acknowledge the support of the CERN management and staff and the skill and effort of the technicians of our collaborating institutes. Special thanks go to V. Anosov and V. Pesaro for their technical support during the installation and the running of this experiment.

References

[1] D. de Florian, R. Sassot, M. Stratmann, W. Vogelsang, Phys. Rev. Lett. **101** (2008) 072001; Phys. Rev. **D80** (2009) 034030.
[2] New Muon Collaboration, P. Amaudruz *et al.*, Phys. Rev. Lett. **66** (1991) 2712.
[3] New Muon Collaboration, M. Arneodo *et al.*, Phys. Rev. **D50** (1994) R1.
[4] HERMES Collaboration, K. Ackerstaff, *et al.*, Phys. Rev. Lett. **81** (1998) 5519.
[5] NA51 Collaboration, A. Baldit, *et al.*, Phys. Lett. **B332** (1994) 244.
[6] E866 Collaboration, R. Towell *et al.*, Phys. Rev. **D64** (2001) 052002.
[7] G. Garvey and J. C. Peng, Prog. Part. Nucl. Phys. **47** (2001) 203.
[8] R. S. Bhalerao, Phys. Rev. **C63** (2001) 025208.
[9] J. C. Peng, Eur. Phys. J. **A18** (2003) 395.
[10] C. Bourrely, J. Soffer and F. Buccella, Eur. Phys. J. **C23** (2002) 487.
[11] E. Leader, A. Sidorov, D. Stamenov, Phys. Rev. **D75** (2007) 074027.
[12] M. Hirai, S. Kumano, N. Saito, Phys. Rev. **D74** (2006) 014015.
[13] S. F. Pate, D. W. McKee and V. Papavassiliou, Phys.Rev. **C78** (2008) 015207.
[14] HERMES Collaboration, A. Airapetian *et al.*, Phys. Rev. **D71** (2005) 012003.
[15] HERMES Collaboration, A. Airapetian *et al.*, Phys. Lett. **B666** (2008) 446.
[16] S. D. Bass and A. W. Thomas, Phys. Lett. **B684** (2010) 216.
[17] COMPASS Collaboration, M. Alekseev *et al.*, Phys. Lett. **B680** (2009) 1.
[18] European Muon Collaboration, J. Ashman *et al.*, Nucl. Phys. **B328** (1989) 180.
[19] Spin Muon Collaboration, B. Adeva *et al.*, Phys. Lett. **B420** (1998) 180.
[20] COMPASS Collaboration, M. G. Alekseev *et al.*, Phys. Lett. **B690** (2010) 466.
[21] COMPASS Collaboration, P. Abbon *et al.*, Nucl. Instrum. Meth. **A577** (2007) 455.
[22] V. Aleksakhin, Y. Bedfer, S. Gerasimov, A. Korzenev, Phys. Part. Nucl. Lett. **4** (2007) 350.
[23] I.V. Akushevich, N. M. Shumeiko, J. Phys. **G20** (1994) 513.
[24] O.A. Rondon, Phys. Rev. **C60** (1999) 035201.
[25] E143 Collaboration, K. Abe *et al.*, Phys. Lett. **B452** (1999) 194.
[26] HERMES Collaboration, A. Airapetian *et al.*, Phys. Rev. **D75** (2007) 012007.
[27] S. Neliba *et al.*, Nucl. Instrum. Meth. **A526** (2004) 144.
[28] J. Ball *et al.*, Nucl. Instrum. Meth. **A498** (2003) 101.
[29] A. D. Martin, W. J. Stirling, R. S. Thorne, Phys.Lett. **B636** (2006) 259.
[30] D. de Florian, R. Sassot, M. Stratmann, Phys. Rev. **D75** (2007) 114010.
[31] R. Machleidt *et al.*, Phys. Rep. **149** (1987) 1.
[32] European Muon Collaboration, M. Arneodo *et al.*, Nucl. Phys. **B321** (1989) 541.
[33] M. Wakamatsu, Phys. Rev. **D67** (2003) 034005.
[34] C. Bourrely, J. Soffer, F. Buccella, Phys.Lett. **B648** (2007) 39.
[35] COMPASS Collaboration, V. Yu. Alexakhin *et al.*, Phys. Lett. **B647** (2007) 8.
[36] A. Sissakian, O. Shevchenko, O. Ivanov, Eur. Phys. J. **C65** (2010) 413.

[37] COMPASS Collaboration, M. Alekseev *et al.*, Phys. Lett. **B660** (2008) 458.

[38] M. Wakamatsu, "Flavor asymmetry of the polarized sea-quark distributions in the proton", arXiv:1003.2457v1 [hep-ph]

[39] S. Kumano and M. Miyama, Phys. Rev. **D65** (2002) 034012.

Table 1: Unfolded asymmetries for charged pions and kaons produced on a proton target. The first error is statistical, the second is systematic.

$\langle x \rangle$	$\langle Q^2 \rangle$ $(\mathrm{GeV}/c)^2$	$A_{1,p}^{\pi+}$	$A_{1,p}^{\pi-}$	$A_{1,p}^{K+}$	$A_{1,p}^{K-}$
0.0052	1.16	$0.008 \pm 0.029 \pm 0.016$	$0.020 \pm 0.029 \pm 0.016$	$0.078 \pm 0.067 \pm 0.038$	$-0.112 \pm 0.069 \pm 0.039$
0.0079	1.46	$0.041 \pm 0.018 \pm 0.010$	$0.016 \pm 0.018 \pm 0.010$	$0.126 \pm 0.036 \pm 0.021$	$-0.040 \pm 0.039 \pm 0.022$
0.0142	2.12	$0.040 \pm 0.014 \pm 0.008$	$0.049 \pm 0.015 \pm 0.009$	$0.046 \pm 0.028 \pm 0.016$	$0.038 \pm 0.031 \pm 0.018$
0.0245	3.22	$0.122 \pm 0.022 \pm 0.014$	$0.055 \pm 0.023 \pm 0.013$	$0.117 \pm 0.041 \pm 0.024$	$0.092 \pm 0.048 \pm 0.028$
0.0346	4.36	$0.156 \pm 0.030 \pm 0.019$	$0.060 \pm 0.032 \pm 0.018$	$0.196 \pm 0.054 \pm 0.033$	$0.074 \pm 0.066 \pm 0.037$
0.0487	5.97	$0.141 \pm 0.029 \pm 0.018$	$0.118 \pm 0.031 \pm 0.019$	$0.174 \pm 0.051 \pm 0.031$	$0.027 \pm 0.064 \pm 0.036$
0.0765	8.96	$0.230 \pm 0.031 \pm 0.022$	$0.053 \pm 0.033 \pm 0.019$	$0.215 \pm 0.054 \pm 0.033$	$0.029 \pm 0.071 \pm 0.040$
0.121	13.8	$0.243 \pm 0.041 \pm 0.027$	$0.096 \pm 0.047 \pm 0.027$	$0.315 \pm 0.072 \pm 0.044$	$0.212 \pm 0.101 \pm 0.058$
0.172	19.6	$0.392 \pm 0.058 \pm 0.040$	$0.165 \pm 0.066 \pm 0.038$	$0.355 \pm 0.099 \pm 0.059$	$0.195 \pm 0.147 \pm 0.083$
0.240	27.6	$0.518 \pm 0.060 \pm 0.046$	$0.233 \pm 0.069 \pm 0.041$	$0.450 \pm 0.101 \pm 0.063$	$0.264 \pm 0.157 \pm 0.089$
0.341	40.1	$0.549 \pm 0.097 \pm 0.064$	$0.134 \pm 0.113 \pm 0.064$	$0.512 \pm 0.163 \pm 0.097$	$0.375 \pm 0.259 \pm 0.147$
0.480	55.6	$0.871 \pm 0.122 \pm 0.086$	$0.520 \pm 0.142 \pm 0.085$	$0.726 \pm 0.207 \pm 0.124$	$0.654 \pm 0.339 \pm 0.194$

Table 2: Correlation coefficients ρ of the unfolded asymmetries in bins of x.

x-bin	0.004–0.006	0.006–0.01	0.01–0.02	0.02–0.03	0.03–0.04	0.04–0.06	0.06–0.10	0.10–0.15	0.15–0.20	0.2–0.3	0.3–0.4	0.4–0.7
$\rho(A_{1,p}^{\pi+}, A_{1,p})$	0.29	0.34	0.37	0.38	0.39	0.40	0.41	0.42	0.43	0.43	0.45	0.46
$\rho(A_{1,p}^{\pi-}, A_{1,p})$	0.30	0.34	0.37	0.38	0.38	0.39	0.39	0.39	0.38	0.38	0.39	0.40
$\rho(A_{1,p}^{\pi-}, A_{1,p}^{\pi+})$	0.12	0.15	0.17	0.16	0.15	0.16	0.16	0.15	0.16	0.16	0.19	0.20
$\rho(A_{1,p}^{K+}, A_{1,p})$	0.26	0.28	0.28	0.26	0.27	0.28	0.29	0.30	0.29	0.29	0.30	0.30
$\rho(A_{1,p}^{K+}, A_{1,p}^{\pi+})$	−0.17	−0.09	−0.04	−0.02	−0.02	−0.01	−0.02	−0.01	−0.01	−0.02	−0.02	−0.01
$\rho(A_{1,p}^{K+}, A_{1,p}^{\pi-})$	0.03	0.04	0.04	0.05	0.05	0.05	0.05	0.06	0.05	0.05	0.04	0.03
$\rho(A_{1,p}^{K-}, A_{1,p})$	0.12	0.15	0.17	0.17	0.17	0.18	0.17	0.17	0.16	0.16	0.16	0.15
$\rho(A_{1,p}^{K-}, A_{1,p}^{\pi+})$	0.03	0.03	0.04	0.04	0.04	0.04	0.03	0.04	0.02	0.03	0.02	0.05
$\rho(A_{1,p}^{K-}, A_{1,p}^{\pi-})$	−0.16	−0.09	−0.05	−0.03	−0.03	−0.03	−0.03	−0.03	−0.02	−0.03	−0.04	−0.02
$\rho(A_{1,p}^{K-}, A_{1,p}^{K+})$	0.05	0.08	0.10	0.10	0.10	0.11	0.11	0.12	0.11	0.11	0.13	0.16

Table 3: Corrections to the deuteron spin asymmetries $A_{1,d}^h$ and $A_{1,d}$ due to admixture of ^{7}Li and ^{1}H into the ^{6}LiD target material. The corrections are to be subtracted from the values of Ref. [17].

x range	π^+	π^-	K^+	K^-	incl.
0.004–0.006	0.001	0.	0.001	0.	0.
0.006–0.010	0.001	0.	0.001	0.	0.001
0.010–0.020	0.001	0.001	0.002	0.	0.001
0.020–0.030	0.002	0.001	0.002	0.001	0.001
0.030–0.040	0.002	0.001	0.003	0.001	0.002
0.040–0.060	0.003	0.001	0.003	0.001	0.002
0.060–0.100	0.004	0.002	0.005	0.002	0.003
0.100–0.150	0.006	0.002	0.006	0.003	0.004
0.150–0.200	0.008	0.003	0.008	0.004	0.006
0.200–0.300	0.011	0.004	0.010	0.005	0.008
0.300–0.400	0.015	0.005	0.013	0.009	0.011
0.400–0.700	0.020	0.006	0.017	0.013	0.015

Table 4: First moments of the quark helicity distributions at $Q_0^2 = 3$ (GeV/c)^2 truncated to the range of the measurements and derived with the DSS fragmentation functions. The first error is statistical, the second one systematic. The values of the sea quark distributions for $x \geq 0.3$ are assumed to be zero.

x range	$0.004 < x < 0.3$	$0.004 < x < 0.7$
Δu	$0.47 \pm 0.02 \pm 0.03$	$0.69 \pm 0.02 \pm 0.03$
Δd	$-0.27 \pm 0.03 \pm 0.02$	$-0.33 \pm 0.04 \pm 0.03$
$\Delta\overline{u}$	$0.02 \pm 0.02 \pm 0.01$	—
$\Delta\overline{d}$	$-0.05 \pm 0.03 \pm 0.02$	—
$\Delta s(\Delta\overline{s})$	$-0.01 \pm 0.01 \pm 0.01$	—
Δu_v	$0.46 \pm 0.03 \pm 0.03$	$0.67 \pm 0.03 \pm 0.03$
Δd_v	$-0.23 \pm 0.05 \pm 0.02$	$-0.28 \pm 0.06 \pm 0.03$
$\Delta\overline{u} - \Delta\overline{d}$	$0.06 \pm 0.04 \pm 0.02$	—
$\Delta\overline{u} + \Delta\overline{d}$	$-0.03 \pm 0.03 \pm 0.01$	—
$\Delta\Sigma$	$0.15 \pm 0.02 \pm 0.02$	$0.31 \pm 0.03 \pm 0.03$

Table 5: Full first moments of the quark helicity distributions at $Q_0^2 = 3$ (GeV/c)^2. The unmeasured contributions at low and high x were estimated by extrapolating the data towards $x = 0$ and $x = 1$ and by using the DSSV parameterisation [1]

	Extrapolation	DSSV
Δu	$0.71 \pm 0.02 \pm 0.03$	$0.71 \pm 0.02 \pm 0.03$
Δd	$-0.34 \pm 0.04 \pm 0.03$	$-0.35 \pm 0.04 \pm 0.03$
$\Delta\overline{u}$	$0.02 \pm 0.02 \pm 0.01$	$0.03 \pm 0.02 \pm 0.01$
$\Delta\overline{d}$	$-0.05 \pm 0.03 \pm 0.02$	$-0.07 \pm 0.03 \pm 0.02$
$\Delta s(\Delta\overline{s})$	$-0.01 \pm 0.01 \pm 0.01$	$-0.05 \pm 0.01 \pm 0.01$
Δu_v	$0.68 \pm 0.03 \pm 0.03$	$0.68 \pm 0.03 \pm 0.03$
Δd_v	$-0.29 \pm 0.06 \pm 0.03$	$-0.28 \pm 0.06 \pm 0.03$
$\Delta\Sigma$	$0.32 \pm 0.03 \pm 0.03$	$0.22 \pm 0.03 \pm 0.03$